

Table S1. Fractional atomic coordinates and isotropic displacement parameters ( $\text{\AA}^2$ ) of  $\text{HoCr}_3(\text{BO}_3)_4$ .

Atom	<i>x</i>	<i>y</i>	<i>z</i>	<i>B</i> <sub>iso</sub>	<i>Occ.</i>
Ho	0	0.03019(17)	0.25	0.981(75)	1
Cr1	0	0.58465(37)	0.25	1.118(98)	1
Cr2	0.05642(36)	0.25	0.52700(32)	0.951(71)	1
B1	0.2039(26)	0.2936(22)	0.2216(16)	1.40(23)	1
B2	0.2461(27)	0.0400(26)	0.0073(15)	1.40(23)	1
O1	0.1975(12)	0.5481(11)	0.73195(67)	0.86(10)	1
O2	0.2535(12)	0.1196(12)	0.50207(72)	0.86(10)	1
O3	0.0654(13)	0.23621(88)	0.13919(85)	0.86(10)	1
O4	0.3876(13)	0.1068(11)	0.07888(82)	0.86(10)	1
O5	0.3448(13)	0.23813(99)	0.2876(10)	0.86(10)	1
O6	0.3953(12)	0.4079(11)	0.07744(89)	0.86(10)	1

Table S2. Main bond lengths ( $\text{\AA}$ ) of  $\text{HoCr}_3(\text{BO}_3)_4$ .

Ho—O1 <sup>i</sup>	2.3125(74)	Ho—O2 <sup>ii</sup>	3.1402(81)
Ho—O3 <sup>ii</sup>	2.4320(86)	Ho—O5 <sup>ii</sup>	3.1630(80)
Ho—O5 <sup>iii</sup>	3.0620(91)	Ho—O6 <sup>iii</sup>	2.2495(99)
Cr1—O1 <sup>iv</sup>	1.9711(88)	Cr1—O3 <sup>v</sup>	3.4623(78)
Cr1—O4 <sup>v</sup>	1.9347(90)	Cr1—O5 <sup>v</sup>	1.9590(89)
Cr2—O1 <sup>vi</sup>	3.4757(88)	Cr2—O2 <sup>vii</sup>	1.9781(90)
Cr2—O2 <sup>i</sup>	1.9542(90)	Cr2—O3 <sup>ii</sup>	1.8924(98)
Cr2—O4 <sup>ii</sup>	3.4820(83)	Cr2—O4 <sup>viii</sup>	2.0214(91)
Cr2—O5 <sup>i</sup>	2.061(11)	Cr2—O6 <sup>iii</sup>	3.497(10)
Cr2—O6 <sup>viii</sup>	2.0738(90)	B1—O1 <sup>ix</sup>	1.505(23)
B1—O3 <sup>vii</sup>	1.326(19)	B1—O5 <sup>vii</sup>	1.243(19)
B2—O2 <sup>x</sup>	1.514(27)	B2—O4 <sup>vii</sup>	1.321(20)

Symmetry codes: (i)  $-x+1/2, -y+1/2, -z+1$ ; (ii)  $-x, y, -z+1/2$ ; (iii)  $-x+1/2, y+1/2, -z+1/2$ ; (iv)  $-x, -y+1, -z+1$ ; (v)  $-x+1/2, y+1/2, -z+1/2$ ; (vi)  $-x+1/2, y+1/2, -z+3/2$ ; (vii)  $x, y, z$ ; (viii)  $x+1/2, -y+1/2, z+1/2$ ; (ix)  $x, -y+1, z+1/2$ ; (x)  $x, -y, z+1/2$ ; (xi)  $-x+1/2, -y+1/2, -z$

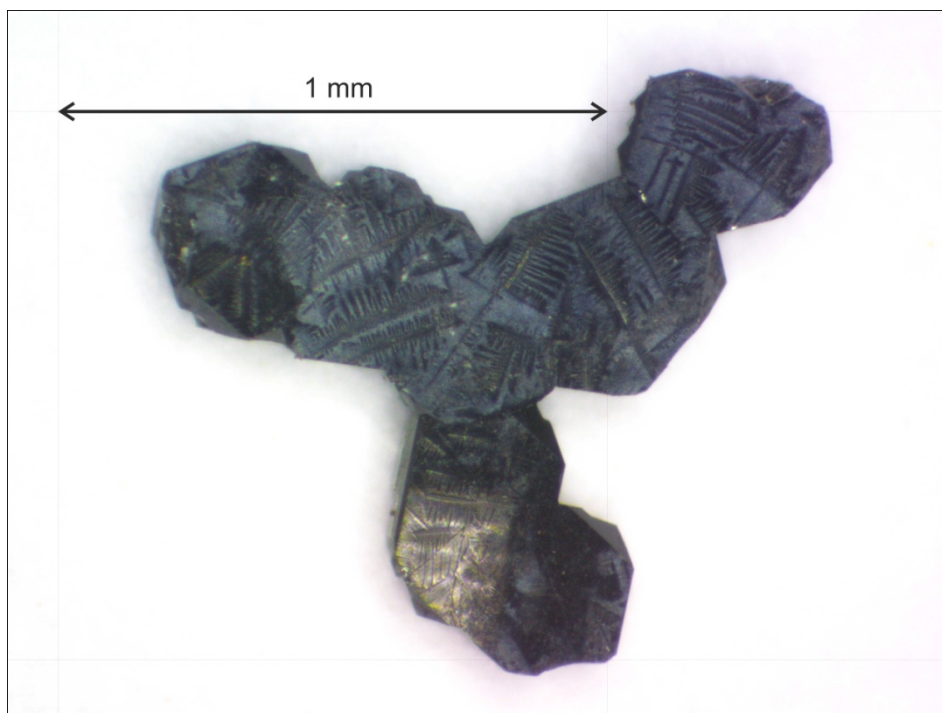
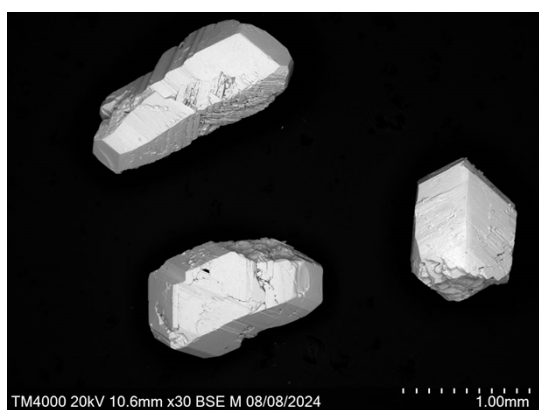
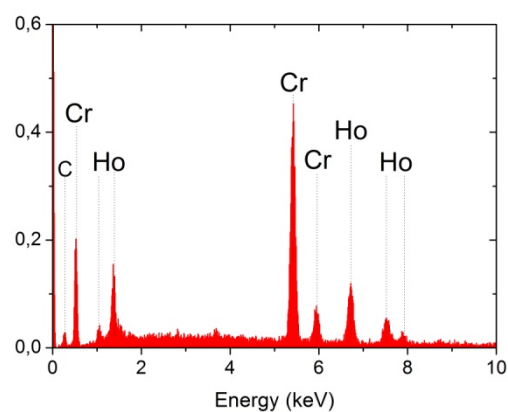


Figure S1. As grown druse of  $\text{CrBO}_3$  crystals.

Figure S2. Microphotography (a) and EDX spectrum of  $\text{HoCr}_3(\text{BO}_3)_4$  (b).



*a*



*b*

Figure S2. Microphotography (a) and EDX spectrum of  $\text{HoCr}_3(\text{BO}_3)_4$  (b).

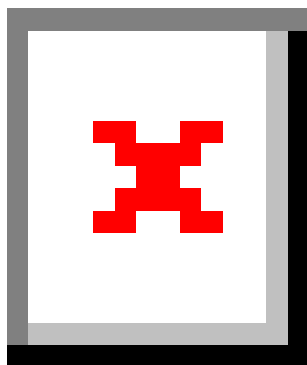


Figure S3. Obtained single crystals during research process (the structural parameters of the phases are presented in Table 4): (a)  $p = 0.011$  joint crystallization of  $\text{Cu}_2\text{CrBO}_5$  and  $\text{CuO}$ ; (b)  $p = 0.055$  –  $\text{CuO}$ ; (c)  $p = 0.099$  –  $\text{CuO}$ ; (d)  $p = 0.143$  –  $\text{CuO}$ ; (e) and (f)  $\text{Cu}^+\text{CrO}_2$ .

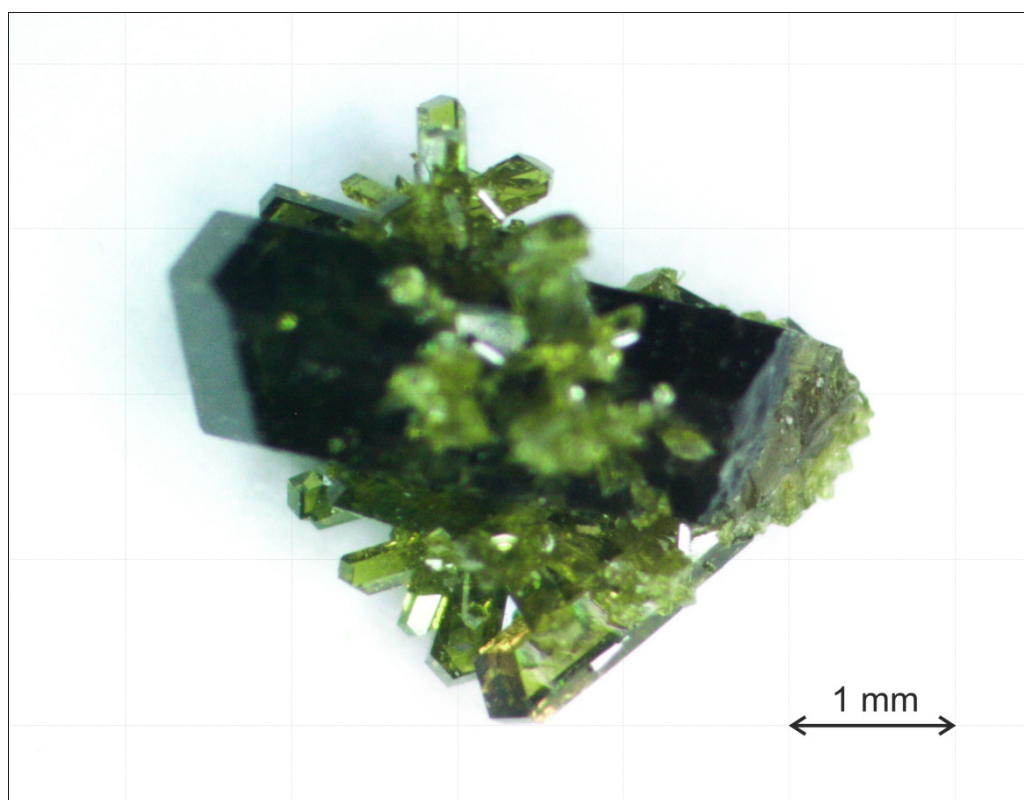


Figure S4. As grown druse of  $\text{HoFe}_3(\text{BO}_3)_4$  crystals.

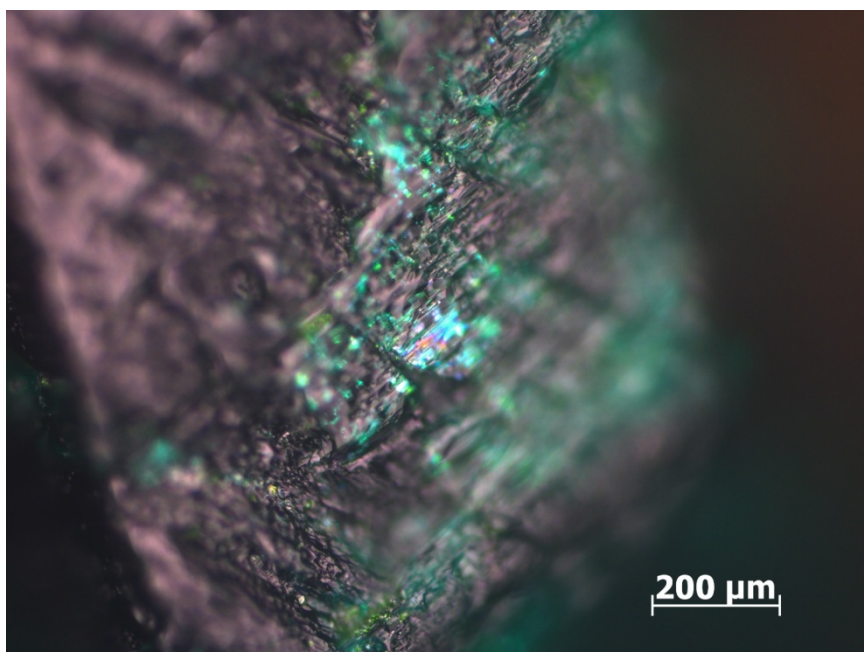


Figure S5. Microphotography of the grown  $\text{HoCr}_3(\text{BO}_3)_4$  crystal.

## The detailed description of STA of $\text{Cu}_2\text{CrBO}_5$ and $\text{HoCr}_3(\text{BO}_3)_4$ samples

The complex superposition pattern of the endothermic and exothermic peaks in a region of 670-780°C is observed at heating of  $\text{Cu}_2\text{CrBO}_5$  polycrystalline sample (Fig. 7c). At  $T = 671^\circ\text{C}$  the melting was began and next the restructuring of this material was follow evidenced by the number of peaks at 722 and 770°C. While the temperature was increased the next stage of melting starting at  $T = 794^\circ\text{C}$  was registered. Following that the exothermal peaks at 819°C and 830°C were appear. Further temperature increasing led to significant heat release possibly related to the recrystallization of the material. The maxima of these processes correspond to 900°C and 960°C. There is a small melting peak at  $T \approx 970^\circ\text{C}$  followed by the stronger melting of the material. The end of this process was not fixed due to the upper temperature constrains. At cooling there are exothermic peaks only (blue line in Fig. 7c).

No endothermic peaks was fixed in DSC curve of  $\text{Cu}_2\text{CrBO}_5$  crystal (Fig. 7b). However there is a number of exothermic peaks in the region of 670-970°C. Like the polycrystalline one this dependences show the start of the melting process at  $T \approx 1030^\circ\text{C}$ . At cooling the exothermic peaks corresponding to crystallization were found. The weight of the samples didn't change during the measurements. Microphotographies of the single crystal samples after annealing are shown in Fig. S6a, b. It is seen the surface of the crystal went bad and the other crystals appear around. EDX analysis confirmed the presence of the solvent from the crystal inside that led to change of the crystal composition near the surface. The polycrystalline samples staid stable, clean and smooth after annealing (Fig. S6c). So the small crystals contain no flux reminder.

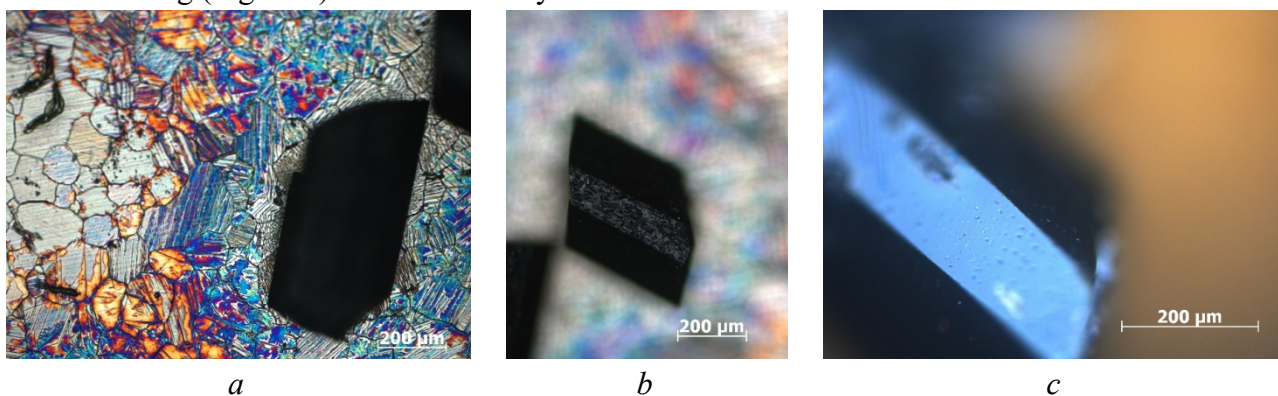


Figure S6. Microphotographies of the single crystal (a, b) and small crystal from the polycrystalline sample (c) after annealing up to 1050°C.

DSC curve of  $\text{HoCr}(\text{BO}_3)_4$  crystal is shown in Fig. 7a. The endothermic peak getting started at  $T = 620^\circ\text{C}$  has stretched out up to 940°C. This process corresponds to melting of the solvent. Further increasing of the temperature has led to solving of  $\text{HoCr}(\text{BO}_3)_4$  crystal. The process has started at  $T \approx 980^\circ\text{C}$  and continued up to 1050°C. At the cooling the material has crystallized due to the presence of exothermic peak in the range of 780-1000°C.